Modeling of postseismic deformation following the 2019 Ridgecrest earthquake sequence

Kang Wang* and **Roland Bürgmann**

Berkeley Seismology Lab. - UC Berkeley

*Email: kwang@seismo.berkeley.edu

Poster# 115

Coseismic slip model

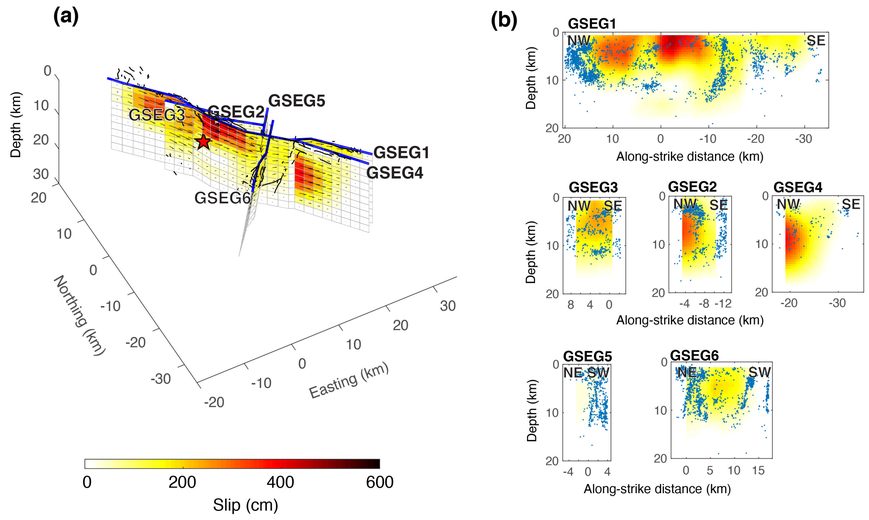

Figure 1. Coseismic slip model of the 2019 Ridgecrest earthquake sequence inverted from static GNSS and Sentinel-1 InSAR data (Wang et al., 2020). (a) Slip distribution in a 3D perspective. (b) Slip distribution along average strike of the different fault segments. Dots are relocated aftershocks within 1 km from model surface trace during ~5 days after the Mw 6.4 foreshock on 4 July 2019 (Shelly, 2020).

Postseismic InSAR observations

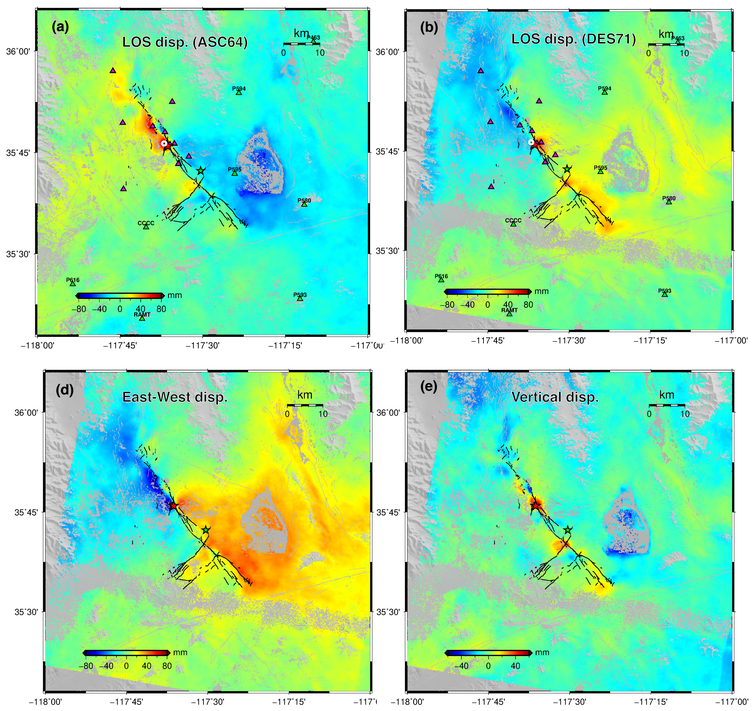

Figure 2. InSAR observations of postseismic deformation following the 2019 Ridgecrest earthquake sequence. (a) and (b) cumulative line-of-sight (LOS) displacements one year after the mainshock derived from Sentinel-1 data of the ascending track ASC64, and descending track D071, respectively. (c) time series of LOS displacments at a point near the Mw 7.1 mainshock epicenter (white circle in panel a and b). (d) and (e) show the cumulative postseismic displacements along the East-West and Vertical directions, respectively, by decomposing the LOS displacements from both the ascending and descending tracks.

Postseismic GNSS observations

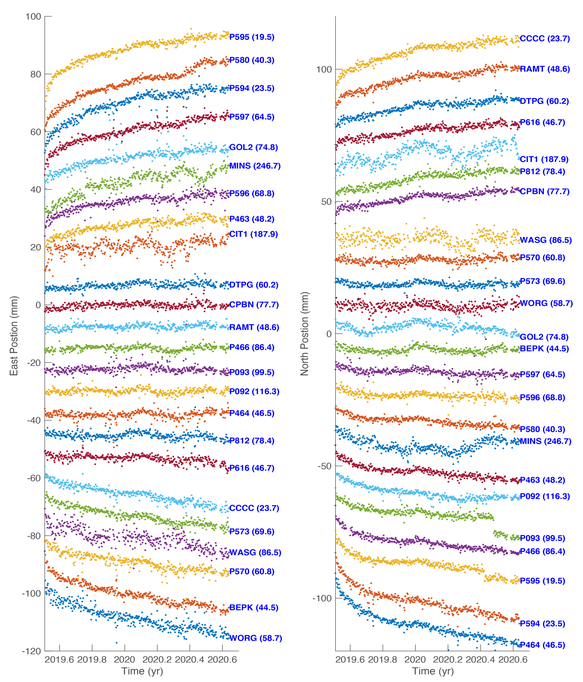

Figure 3. GNSS time series of postseismic deformtion following the 2019 Ridgecrest earthquake. For each site, we estimate the interseismic rate by using data from 2 years before the 2019 Ridgecrest earthquake, to reduce the bias due to the long-lasting postseismic deformation following the 1992 Landers and the 1999 Hector Mine events. Numbers in parentheses denote the distance of the respective GNSS site to the epicenter of the mainshock. The resulting time series is then fit with a logarithm function to estimate the cumulative displacement during a given time period (e.g. 1 year in the afterslip inversion shown in Figure 4-5).

Modeling of postseismic deformation

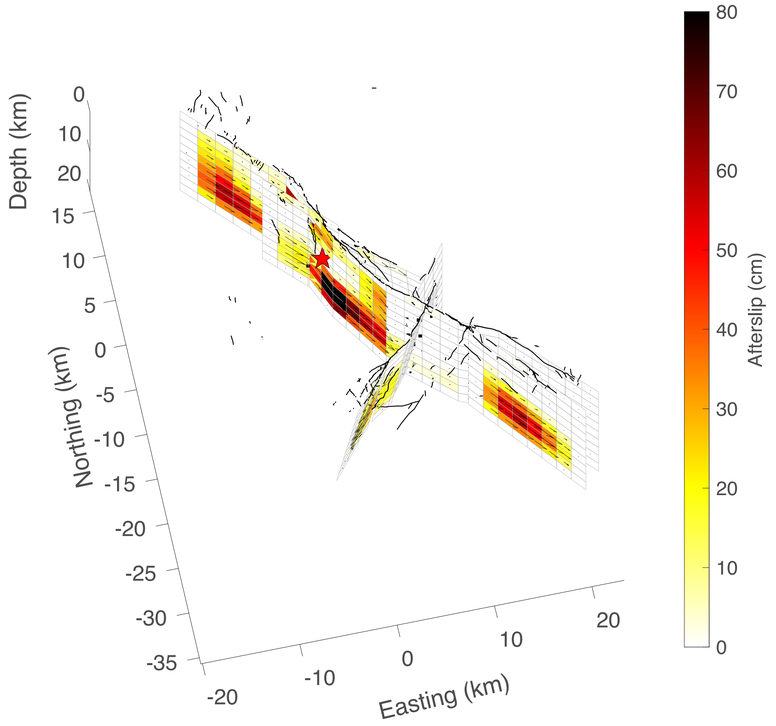

Figure 4. Cumulative afterslip following the 2019 Ridgecrest earthquake sequence derived from the inversion of InSAR and GNSS data one year after the mainshock using a fault geometry that is the same as the coseismic slip model shown in Figure 1. Compared to the coseismic slip model, most afterslip appears to occurr predominately at the bottom of the fault, despite large uncertainty.

Figure 5. Fitting of GNSS data using the afterslip model shown in Figure 4. Although the afterslip model can explain the near-field GNSS data reasonably well, the model systematically underpredicts the GNSS displacements in the far field, showing that some deep processes, that is viscoelastic relaxation from the lower crust and/or upper mantle, are required to explain the far-field postseismic deformation. Future work will include developing joint models that consider afterslip, poroelastic rebound and viscoelastic relaxation to study the stress evolution following the 2019 events and rheologial structure of East California Shear Zone.

Conclusions and Discussion

- Inversions of geodetic data reveal complex ruptures during the 2019 Ridgecrest earthquake sequence.
- Near-field early postseismic deformation of the 2019 Ridgecreat earthquake is indicative of both poro-elastic rebound and deep afterslip.
- Far-field GNSS postseismic measurements are indicative of viscoelatic relaxation in the lower crust and/upper mantle.

References

Wang and Bürgmann (2020). *Seismo. Res. Lett.* **91** (4): 1998–2009 doi: 10.1785/0220190299

Wang et al. (2020). *Bull. Seismol. Soc. Am.,* **110** (4): 1603–1626 doi: 10.1785/0120200108

Shelly (2020), *Seismo. Res. Lett.* **91** (4): 1971–1978 doi: 10.1785/0220190309